

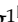


Research Paper

Acetyl-11-keto- β -boswellic acid attenuates titanium particle-induced osteogenic inhibition via activation of the GSK-3 β / β -catenin signaling pathway

Longbin Xiong^{1,2*}, Yu Liu^{1*}, Feng Zhu^{1*}, Jiayi Lin^{1*}, Dongxiang Wen^{1,2}, Zhen Wang³, Jiaxiang Bai¹, Gaoran Ge¹, Congxin Xu¹, Ye Gu⁴, Yaozeng Xu¹, Jun Zhou¹, Dechun Geng¹

1. Department of Orthopaedics, The First Affiliated Hospital of Soochow University, Suzhou, 215006, China;
2. Sun Yat-sen University Cancer Center; State key laboratory of Oncology in South China; Collaborative Innovation Center for Cancer Medicine, Guangzhou, Guangdong 510000, China;
3. Department of Orthopaedics, Suzhou Kowloon Hospital Shanghai Jiao Tong University School of Medicine, Suzhou, Jiangsu 215006, China;
4. Department of Orthopedics, Soochow University Affiliated First People's, Hospital of Changshou City, Changshu, China

*Contributed equally to this work

 Corresponding authors: Dechun Geng, M.D, Ph.D (E-mail: szgengdc@163.com); Jun Zhou, M.D, Ph.D (E-mail: royf1@163.com); Yaozeng Xu, M.D, Ph.D (xuyaozeng@suda.edu.cn)

© The author(s). This is an open access article distributed under the terms of the Creative Commons Attribution License (<https://creativecommons.org/licenses/by/4.0/>). See <http://ivyspring.com/terms> for full terms and conditions.

Received: 2019.04.23; Accepted: 2019.09.01; Published: 2019.09.23

Abstract

Rationale: Peri-prosthetic osteolysis (PPO) is mainly induced by wear particles and represents the leading cause of implant failure and revision surgery. Previous studies have identified mitigation of wear particle-induced inflammation and bone resorption as the main approaches to treat PPO. Recently, wear particle-induced reduction of bone formation around the prosthesis was identified as a major factor in the development of PPO. Acetyl-11-keto- β -boswellic acid (AKBA), a derivative of frankincense, has been shown to play a potential role in bone metabolism. However, whether AKBA enhances bone formation in wear particle-induced osteolysis remains unknown. In this study, we examined whether AKBA attenuates titanium particle-induced osteogenic reduction.

Methods: Titanium particles were used to induce osteolysis in murine calvaria, and micro-CT and histological analyses were used to evaluate the results. Mouse osteoblast cells, MC3T3-E1 were co-cultured with titanium particles to determine their effect on osteoblast formation *in vitro*.

Results: We demonstrated that AKBA treatment significantly inhibited titanium particle-induced osteogenic inhibition by enhancing osteogenesis both *in vivo* and *in vitro*. AKBA treatment also enhanced the phosphorylation of GSK-3 β , decreased the degradation of β -catenin, and increased the translocation of β -catenin from the cytoplasm to the nucleus. Taken together, these results showed that AKBA treatment attenuated titanium-induced osteogenic inhibition by activating the GSK-3 β / β -catenin signaling pathway.

Conclusion: These findings suggest that AKBA is a promising new target in the prevention and treatment of PPO.

Key words: acetyl-11-keto- β -boswellic acid, peri-prosthetic osteolysis, titanium particle, bone formation, GSK-3 β

Introduction

Peri-prosthetic osteolysis (PPO) induced by wear particles is the primary cause of aseptic prosthesis loosening, which directly affects the service life of implants [1]. More than three-quarters of total joint arthroplasty (TJA) implant loosening is due to aseptic

osteolysis [2]. Wear particles gather at the interface between the bone and implant, resulting in the stimulation of macrophages and fibroblasts and the secretion of inflammatory transmitters, such as tumor necrosis factor- α (TNF- α), prostaglandin E₂,

interleukin 1 β (IL-1 β), and IL-6 [3]. Secreted cytokines act on macrophages, osteoblasts, and osteoclasts and interfere with the RANKL/RANK/OPG signaling pathway, enhancing osteoclasts and weakening osteogenesis. The imbalance between osteoblastic bone formation and osteoclastic bone resorption ultimately leads to PPO [4-6]. Osteoclasts have been recognized as a major factor underlying wear particle-induced osteolysis; however, many studies have recently identified wear particles as the main cause of osteogenic inhibition [7-10]. Wear particles directly impair the expression of various collagens, alkaline phosphatase (ALP) activity, osteogenic differentiation and mineralization in osteoblasts [8, 9, 11, 12]. Besides, the chemokines and cytokines like IL-1, IL-6, TNF- α , and PGE-2 secreted by macrophages suppress osteoblastic function [10, 13-15]. Moreover, osteogenic reduction in titanium-induced osteolysis might be regulated via the Wnt and BMP signaling pathway [16, 17]. Therefore, triggering the promotion of osteogenesis could be a promising therapy in the treatment of PPO.

Frankincense is a hard, gelatinous resin exudate found in the trunks of trees belonging to the olive family [18]. It is extensively used as a medicinal material in Chinese traditional medicine and Ayurvedic medicine in India [19, 20]. The primary chemical constituents of frankincense are terpenoids, volatile oils, arabinose, and xylose, which are collectively known as boswellic acid (BA) compounds due to their carboxyl structures. The main active ingredients in frankincense are α -boswellic acid (α -BA), β -boswellic acid (β -BA), β -BA-derivative acetyl-boswellic acid (ABA), 11-keto- β -boswellic acid (KBA), and acetyl-11-keto- β -boswellic acid (AKBA), among which AKBA is the most active and widely used [21, 22]. Several studies have shown that AKBA has anti-inflammatory, anti-tumor, anti-ulcer, anti-asthma, anti-oxidation, analgesic, immunomodulatory, and lipid regulatory effects [23-26]. However, relatively few studies have explored the effect of AKBA on bone metabolism. Takada and coworkers found that AKBA enhanced osteoclast apoptosis and suppressed osteoclastogenesis by inhibiting the NF- κ B signaling pathway [27]. Recently, Bai et al. found an association between AKBA treatment and osteoblast differentiation [28]. These findings assumed that AKBA was involved in the regulation of bone tissue; whether AKBA regulated bone formation in titanium-induced osteolysis was unclear.

In this study, we explored the relationship between AKBA treatment and titanium-induced osteogenic reduction. We used titanium particles to induce osteolysis in murine calvaria *in vivo* and

incubated them with MC3T3 cells *in vitro*. Our results demonstrated that AKBA treatment promoted bone regeneration following osteolysis induced by titanium particles. The bone regeneration occurred through the AKBA-mediated activation of the GSK-3 β / β -catenin signaling pathway and promotion of osteogenic differentiation. Taken together, these results indicate that AKBA is a promising pharmaceutical therapy for the prevention and treatment of PPO.

Materials and Methods

Titanium particle preparation

Titanium particles, which were used to stimulate osteolysis, were purchased from Alfa Aesar (#00681, Ward Hill, MA, USA) and processed by Powder-Tech Associates, Inc. (North Andover, MA, USA). Over 95% of the titanium particles had circle diameters smaller than 4 μ m. Endotoxins were removed by calcining at 180°C for 12 h and then rinsing in 75% ethanol for 48 h. The concentration of endotoxins in the particles was detected using a Limulus Amoebocyte Lysate assay detection kit (LAL, Biowhittaker, Walkersville, MD, USA). Endotoxin standard (0.1, 0.25, 0.5, 1.0 EU/ml) or 50 μ l of the sample (0.1 mg/ml titanium particles after endotoxin removal) were dispensed into the endotoxin-free reaction tubes and incubated in 37°C water bath. Each series of determinations included a blank (50 μ l of LAL Reagent Water) plus the four endotoxin standards run in duplicate. Subsequently, 50 μ l of LAL and 100 μ l of substrate solution (prewarmed 37°C) were added. The reaction was terminated after 10 min by adding 100 μ l of stop reagent, and the particles were removed by centrifugation (1200 rpm for 10 min). Subsequently, 200 μ l solution from each tube was transferred to a 96-well plate and the absorbance was read at 405 nm. Finally, concentrations of endotoxin were calculated by using a standard curve, and only samples with endotoxin levels <0.02 EU/mL were used [29].

Animal studies and drug application

A titanium-induced mouse calvaria model was generated as previously described [30, 31]. All protocols met the requirements of the National Institutes of Health (NIH) Guide for the Care and Use of Laboratory Animals and the guidelines for animal treatment of the First Affiliated Hospital of Soochow University (approval number: 201709A472). Briefly, 40 eight-week-old male C57BL/6 mice were randomly divided into four groups (n=10/group): (1) sham operation group, treated with physiological saline, (2) model group, treated with 20 mg titanium particles in physiological saline, (3) low AKBA treatment group in which model group mice were treated with 5 mg/kg per day AKBA, and (4) high AKBA treatment group in

which model group mice were treated with 20 mg/kg per day AKBA. After anesthetizing and preparing the skin, an incision was made in the middle of the calvaria. In the sham operation group, the surgical incision was stitched closed without additional intervention. In the other groups, 20 mg titanium particles were evenly injected under the periosteum of the biparietal suture. AKBA (Sigma-Aldrich, St. Louis, MO, USA) was dissolved in dimethyl sulfoxide (DMSO) and diluted in physiological saline, and each group received the same amount of DMSO. After 2 days, either physiological saline or AKBA was administered to the model and AKBA groups, respectively, via gastric infusion once a day for two weeks.

Micro-computed tomography (micro-CT) analysis

The mice were sacrificed after two weeks by cervical dislocation, and the calvaria (n=5/group) were collected and fixed in 4% paraformaldehyde. Surface erosion in the calvaria was measured using Micro-CT (SkyScan1176, Aartselaar, Belgium). The scanning parameter of the isometric resolution was set at 9 μm , and the X-ray energy was set at 80 kV and 100 mA, according to the manufacturer's instructions. Three-dimensional (3D) image reconstructions were taken, and SkyScan software was used for quantitative analysis. Regions of interest (ROI) of equal area (3 mm in diameter) were identified in the center of each calvaria. SkyScan software was used to analyze bone mineral density (BMD), bone volume (BV), bone volume/tissue volume (BV/TV), and the number of pores in the ROI.

Histological and immunohistochemical analyses

After decalcification in 10% ethylene diamine tetraacetic acid (EDTA, Sigma-Aldrich, St. Louis, MO, USA) for 28 days, the calvaria (n=5/group) were embedded in molten paraffin. The tissues were cut into 6 μm sections and prepared for hematoxylin and eosin (H&E), Masson's trichrome, and tartrate-resistant acid phosphatase (TRAP) staining, following the manufacturer's protocols. Images were captured using an AxioCam HRC microscope (Carl Zeiss, Germany). The bone eroded surface (BES) area ratio and bone thickness (BT) at the closest side of biparietal suture were determined using Image J, and the ratio of osteoclast surface-to- bone perimeter (Oc.S/OB) and the number of osteoclasts to bone surface (N.Oc/BS) were determined using Bioquant Osteo 2017 (BIOQUANT Image Analysis Corporation, Nashville, TN, USA). Blue-colored new bone collagen fiber was observed using Masson's trichrome staining.

Calcein double labeling assay was used to evaluate the dynamic bone formation. Briefly, calcein (Sigma-Aldrich) dissolved in phosphate buffered saline (PBS) was intraperitoneally injected at a concentration of 10 mg/kg on the 1st and 7th days before sacrifice. The calcein double labeling images of undecalcified bone sections were captured using a fluorescence microscope, and mineral apposition rate (MAR) was calculated using Bioquant Osteo 2017.

Expression of alkaline phosphatase (ALP), Osteocalcin (OCN), Osterix, pSer9-GSK-3 β , and β -catenin in the calvaria was detected by immunohistochemistry (IHC) using the corresponding primary antibodies (Abcam, ab95462, ab93876, ab22552, ab131097, ab32572). In brief, the sections were dewaxed with xylene and then subjected to gradient hydration and antigen retrieval with hyaluronidase for 1 h at 37°C and pepsin for 25 min at room temperature. The sections were then blocked with second antibody homologous serum for 30 min. Next, the paraffin sections were incubated with primary antibodies at 4°C. After 12 h, the sections were rinsed with PBS and incubated with secondary antibodies for 30 min at room temperature. A DAB Horseradish Peroxidase Color Development Kit (Beyotime, Shanghai, China) was used to induce the chromogenic reaction. IHC-positive cells, which were dark brown and mainly distributed in the periosteum and laminae superficialis of the bone lamella, were counted using Bioquant Osteo 2017.

Cell culture and osteoblast differentiation

The mouse osteoblast cell line MC3T3-E1 was received from the American Type Culture Collection (ATCC, Rockville, MD, USA). After thawing, MC3T3-E1 cells were cultured in Alpha-Minimum Essential Medium (α -MEM) supplemented with 10% FBS and 1% penicillin/streptomycin at 37°C with 5% CO₂. Osteogenic induction medium consisted of Dulbecco's Modified Eagle Medium (DMEM) supplemented with 10% FBS, 1% penicillin/streptomycin, 100 nM dexamethasone, 10 mM β -glycerophosphate, and 50 mM vitamin C. To simulate the osteolytic microenvironment, 5 $\mu\text{g}/\text{cm}^2$ titanium particles in medium were added to the cells, and the medium was changed every 3 days. The cells were then treated with low (100 nM) or high (1000 nM) concentrations of AKBA in the presence of titanium particles.

Cell viability assay

MC3T3-E1 cells were cultured in 96-well plates for 12 h to ensure cell adhesion. To assess the toxicity of AKBA, titanium particles, and ICG-001 on the cells, various concentrations were added and incubated for

1, 3, or 5 days. To evaluate cell viability, Cell Counting Kit-8 (CCK-8; Beyotime) was used, following the manufacturer's protocols. The MC3T3-E1 inhibition was plotted using GraphPad Prism 7.

Alkaline phosphatase assay

MC3T3-E1 cells were grown in a differentiation-inducing medium for 7 days, and ALP was measured as a phenotypic marker of bone formation. Cells were rinsed 3 times with PBS before fixation in 4% paraformaldehyde at 4°C for 30 min. After washing 3 times with PBS, the cells were incubated in 5-bromo-4-chloro-3-indolyl-phosphate/nitro blue tetrazolium (BCIP/NBT; Beyotime) staining solution for 30 min at room temperature in the dark. ALP-positive cells were counted under a microscope.

Alizarin red S staining

MC3T3-E1 cells were grown in a differentiation-inducing medium for 14 days, washed 3 times with ddH₂O, and then fixed in 95% alcohol for 15 min. The cells were then incubated in Alizarin red S (Sciencell, California, USA) solution for 15 min and washed 3 times with ddH₂O at room temperature before imaging under a microscope. The alizarin red complexed with calcium nodules was dissolved in 5% perchloric acid solution for 30 min at 37°C, and the absorbance was determined at 420 nm.

RNA extraction and quantitative real-time (qRT)-PCR

MC3T3-E1 cells were grown in a differentiation-inducing medium for 24 hours, and total RNA was isolated using Beyozol reagent (Beyotime). The RNA integrity was determined by separating the RNA on an agarose gel and quality was assessed by measuring the A260/A280 and A260/A230 ratio cutoff higher than 1.8 and 2.0, respectively. Two micrograms of total RNA were used for reverse transcription to synthesize cDNA with dNTP mix and RNase-free H₂O, following the manufacturer's protocols. qRT-PCR was performed using SYBR1 Premix Ex Taq™ (Takara, Dalian, Japan). The qRT-PCR parameters were as follows: 95.0°C for 30 s, 39 cycles of 95.0°C for 5 s and 60.0°C for 30 s, and 95.0°C for 10 s, followed by a melt curve from 65.0 to 95.0°C at an increment of 0.5°C per 5 s. Three samples were obtained from three independent experiments, and each sample was analyzed in triplicate. The gene expression data were normalized to an internal control (GAPDH) and were analyzed using the comparative 2^{-ΔΔC_q} method only when amplification efficiency calculated using the standard curve of the mRNAs of interest and the internal mRNA was 90%~110% [32]. GraphPad Prism 7 was used to calculate the data as fold changes compared with the

control group. The primer sequences used are shown in Table 1.

Table 1. Primer sequence

Primer sequence		
mRNA	Forward (5'-3')	Reverse (5'-3')
GAPDH	TGACCTCAACTACATGGTC TACA	CTTCCCATTCTCGGCCTTG
OCN	AAGCAGGAGGGCAAAAAG GT	TTTGTAGCGGCTTCAAGC
Runx2	AGAGTCAGATTACAGATC CCAGG	TGGCTCTTCTACTGAGAGAG G
Osterix	ACCCCAAGATGTCTATAA GCC	CGCTCTAG CTCTGACAGTTG
ALP	GGCTGGAGATGGACAAA TTCC	CCGAGTGGTAGTCACAATGC C
OPN	CACT CCAATCGTCCCTACAGT	CTGGAAACTCCTAGACTTTG ACC
β-catenin	GGAAAGGAGGCACAAAAG AAGC	CCCCTTAGGCACTAGGAGC
Axin-2	ACCAGGATGGTGCATACC TCT	CCCATTACAAGCAAACCAGA AGT

GADPH: glyceraldehyde-3-phosphate dehydrogenase; OCN: osteocalcin; Runx2: runt-related transcription factor 2; ALP: alkaline phosphatase; OPN: osteopontin.

Western blot analysis

MC3T3-E1 cells were grown in a differentiation-inducing medium for 3 days, washed, and then collected with 0.5% trypsin (GIBCO, Grand Island, U.S.). Cells were lysed in radio immunoprecipitation assay (RIPA; Beyotime) buffer for 30 min at 4°C and then the supernatant was collected by centrifugation at 14,800 rpm at 4°C. The supernatant was purified, and total protein concentration quantified using a bicinchoninic acid protein kit (BCA kit; Beyotime). Twenty μg total protein were separated using SDS-PAGE (New Cell & Molecular Biotech Co., Ltd., Suzhou, China) and then transferred to a nitrocellulose filter membrane. After blocking with QuickBlock™ blocking buffer (Beyotime), the membranes were incubated with the appropriate primary antibodies for 12 h at 4°C. Antibodies against Runx2 (1:1000), OCN (1:500), Osterix (1:1000), total GSK-3β (1:2000), pSer9-GSK-3β (1:500), β-catenin (1:5000), and Axin-2 (1:1000) were purchased from Abcam. The membranes were rinsed 3 times with TBS-Tween and then incubated at room temperature with secondary antibody (1:5000) for 1 h. Enhanced chemiluminescence (ECL; Sigma-Aldrich, St. Louis, MO, USA) was used to visualize protein bands, and the relative grey level was analyzed using Image J.

Immunofluorescence assay

MC3T3-E1 cells were grown on coverslips in a differentiation-inducing medium for 4 h. The cells were then rinsed 3 times with PBS, fixed in 4% paraformaldehyde for 15 min, and permeabilized with

0.2% Triton X-100 for 10 min. Coverslips were blocked with serum for 30 min. Cover glasses were subsequently incubated in primary antibodies against β -catenin (1:250) overnight at 4°C. Coverslips were incubated with FITC-conjugated secondary antibody (1:200, ab6785, Abcam) at room temperature for 2 h in the dark. After washing 3 times with PBS, the coverslips were incubated with DAPI for 1 h and mounted to slides using HelixGen anti-fade fluorescence mounting medium (Beyotime). Coverslips were imaged using a fluorescence microscope.

Statistics

The data were presented as means \pm standard deviation (SD), and SDs reflected differences between three independent *in vitro* experiments. GraphPad Prism 7 was used for statistical analysis. Normal distribution was verified before using parametric tests with D'Agostino & Pearson omnibus normality. Statistical significance was determined by one-way ANOVA with the Tukey's multiple comparisons test.

A value of $P < 0.05$ was considered statistically significant.

Results

AKBA treatment attenuated bone loss and enhanced bone formation in titanium-induced osteolysis

Fig. 1A illustrates that titanium particles enhanced bone loss in murine calvaria, which was markedly attenuated by treatment with AKBA. Moreover, the BMD of the model group was significantly decreased compared with that of the sham group (103.0 ± 4.425 mg/mm³ vs. 134.5 ± 4.376 mg/mm³, respectively); the decrease of BMDs of the low (118.8 ± 4.293 mg/mm³) and high (122.1 ± 5.684 mg/mm³) AKBA treatment groups was prevented considerably compared with the model group (Fig. 1B). Also, other parameters, such as the BV, BV/TV, and the number of pores, showed that AKBA eased titanium-induced osteolysis (Fig. 1C–E).

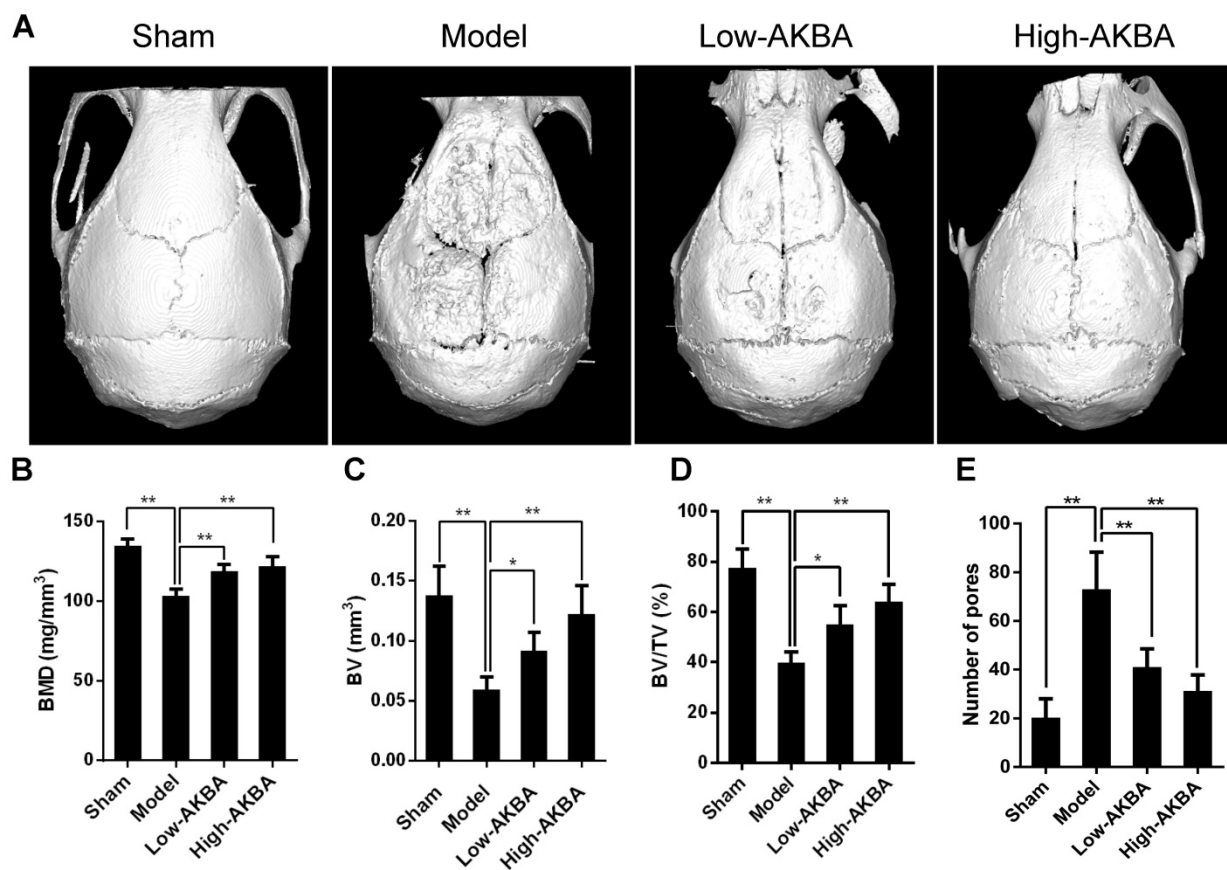


Figure 1. AKBA treatment attenuated titanium particle-induced bone loss and increased bone mass in a murine calvaria model. (A) micro-CT reconstruction images, (B) bone mineral density (BMD, mg/mm³), (C) bone volume (BV, mm³), (D) bone volume/tissue volume (BV/TV, %) and (E) number of pores within the region of interest (ROI). Both low-AKBA (5 mg/kg per day) group and high-AKBA (5 mg/kg per day) group contained 20 mg titanium particles. n=5 per group. Data are presented as means \pm SD. * $P < 0.05$ and ** $P < 0.01$, compared with the model group.

H&E and TRAP staining were performed to further verify the attenuation of osteolysis upon AKBA treatment (Fig. 2A and B). Bone morphometric analysis of H&E staining indicated that AKBA treatment remarkably reduced the ratio of eroded bone surface to bone surface (EBS/BS; Fig. 2E), as well as prevented the decrease of BT (Fig. 2F) from 0.173 ± 0.029 mm in the model group to 0.258 ± 0.020 mm and 0.281 ± 0.031 mm in low and high AKBA treatment groups, respectively. Likewise, the ratio of osteoclast surface-to-bone surface decreased to $8.06\%\pm 0.37\%$ in the low AKBA group and $6.49\%\pm 0.93\%$ in the high AKBA group, compared with

$20.63\%\pm 2.74\%$ in the model group (Fig. 2G). Furthermore, the average number of osteoclasts in the bone surface (N.Oc/BS) was significantly decreased in AKBA-treated mice compared with that in the model group (Fig. 2H).

To observe bone formation in murine calvaria, calcein double labeling and Masson's trichrome staining were performed. The calcein double labeling showed that AKBA treatment significantly enhanced bone formation and increased mineral apposition rate (Fig. 2C&I). Similarly, more new bone collagen fibers were observed in AKBA-treated groups compared to the model group (Fig. 2D).

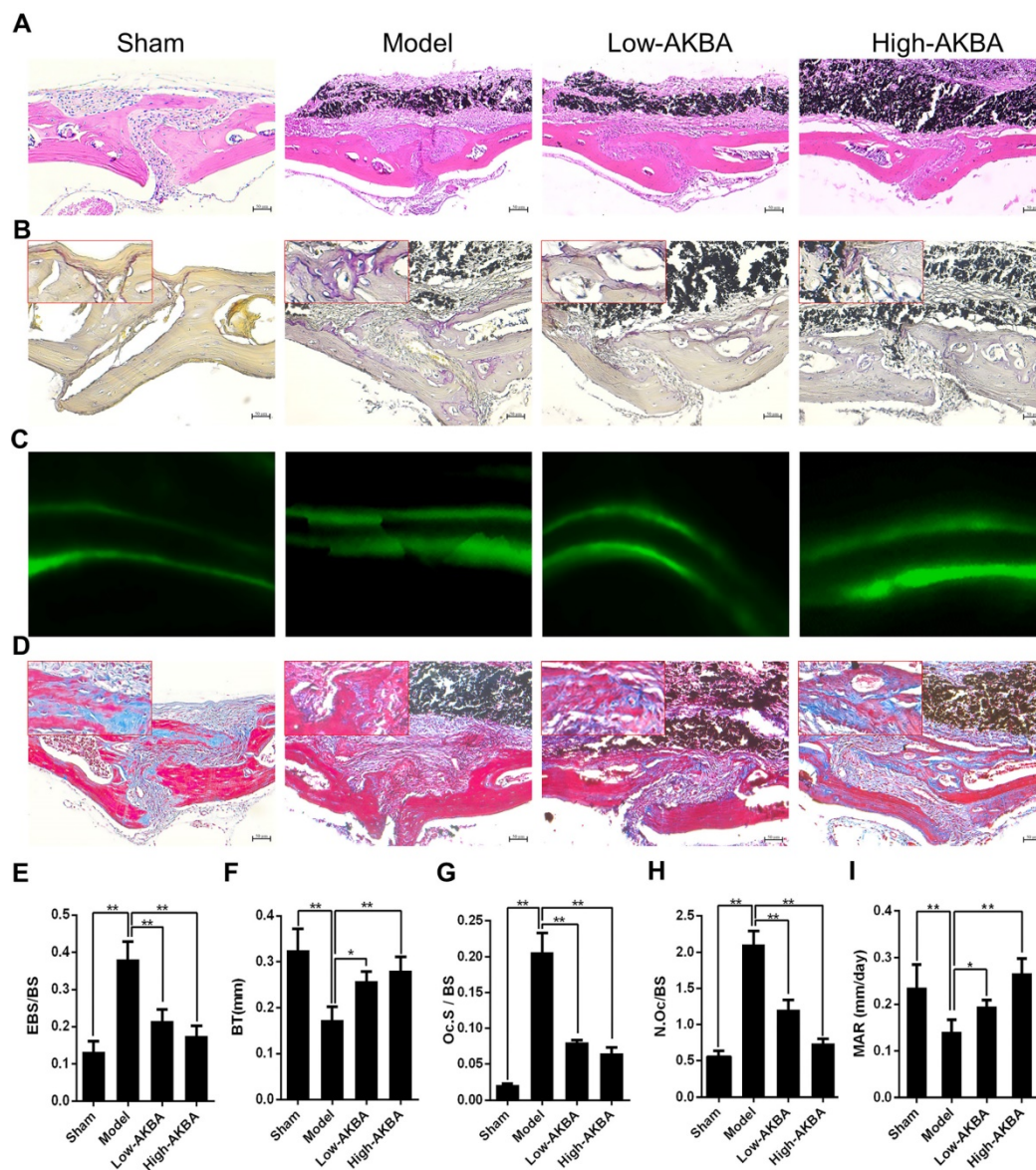


Figure 2. AKBA treatment attenuated titanium particle-induced osteolysis in histological analysis of calvaria sections. (A) H&E staining, (B) TRAP staining, (C) Calcein double labeling, (D) Masson's trichrome staining, blue-colored new bone collagen fibers, (E) the ratio of eroded bone surface to bone surface (EBS/BS), (F) bone thickness (BT, mm), (G) osteoclast surface/bone surface (Oc.S/BS), (H) average number of osteoclasts to bone surface (N.Oc/BS), and (I) mineral apposition rate (MAR). Both low-AKBA (5 mg/kg per day) group and high-AKBA (5 mg/kg per day) group contained 20 mg titanium particles titanium particles. n=5 per group. Scale bar=50 μ m. Data are presented as means \pm SD. * $P<0.05$ and ** $P<0.01$, compared with the model group.

AKBA treatment eased titanium-induced osteolysis by enhancing osteogenesis

To further verify whether AKBA treatment enhanced osteogenesis in titanium-induced osteolysis, IHC staining was used to measure the expression of osteogenic markers. AKBA treatment significantly enhanced osteogenesis in titanium-induced osteolysis, as evidenced by increased expression of the osteogenic markers ALP, Osterix, and OCN (Fig. 3A–C). However, fewer IHC-positive cells were observed in the model group compared with either the sham group or AKBA treatment groups. These results suggested that titanium particles inhibited the

expression of osteogenic markers, while AKBA treatment increased their expression (Fig. 3D–F).

AKBA treatment alleviated titanium-induced osteogenic reduction *in vitro*

The CCK-8 cell viability assay was used to determine whether AKBA, titanium particles, and ICG-001 had any cytotoxic effects on MC3T3-E1 cells. The results indicated that cell viability was unaffected by treatment with concentrations below 10 μM of AKBA (Fig. 4A and D), 10 $\mu\text{g}/\text{cm}^2$ of titanium particles (Fig. 4B and E) and 50 μM of ICG-001 (Fig. 4C and F) over 1, 3, and 5 days.

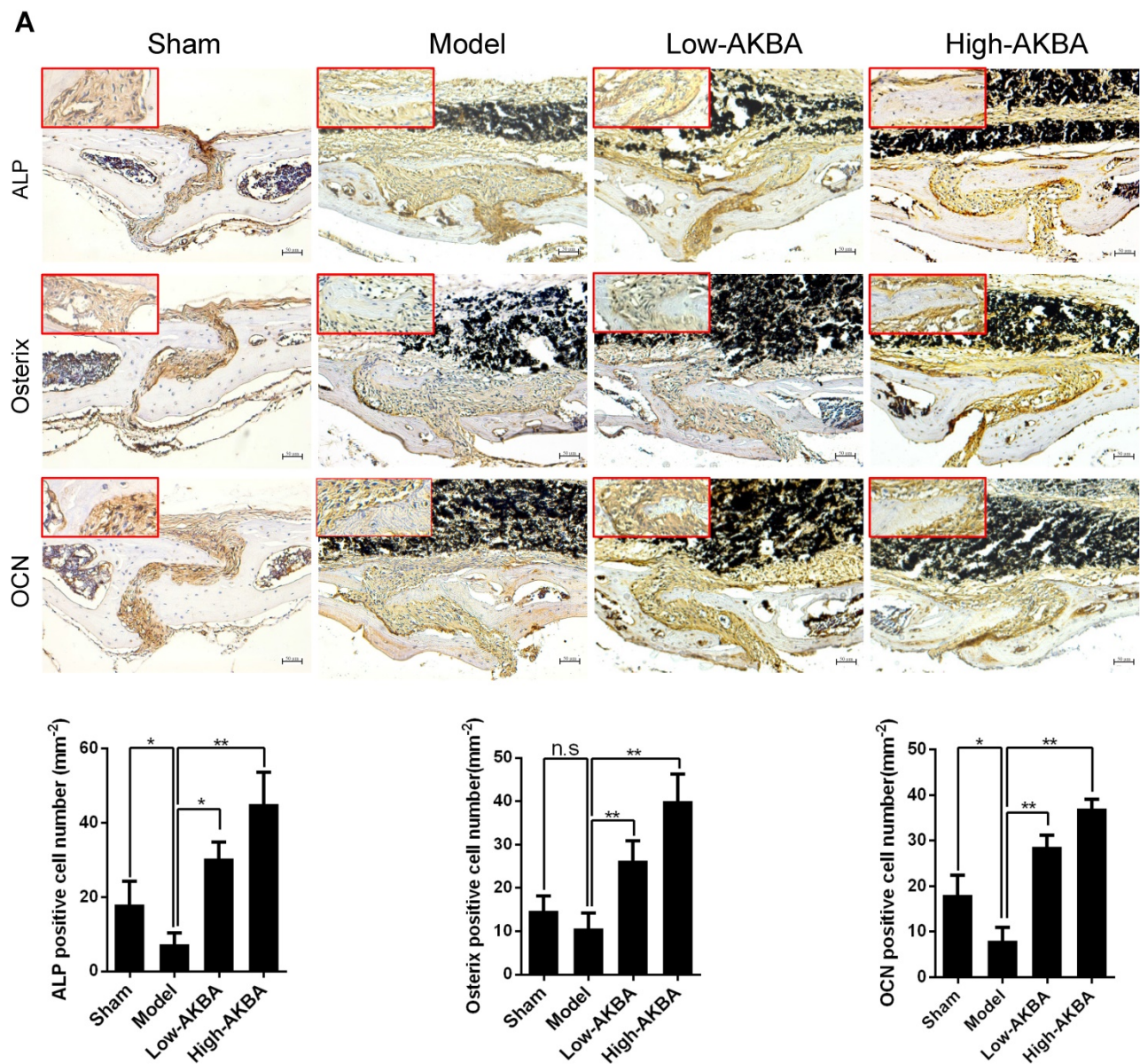


Figure 3. AKBA treatment enhanced new bone regeneration in titanium particle-stimulated osteolysis. (A–C) IHC for ALP, Osterix, and OCN. (D–F) Quantification of the number of positive cells. Both low-AKBA (5 mg/kg per day) group and high-AKBA (5 mg/kg per day) group contained 20 mg titanium particles titanium particles. n=5 per group. Scale bar=50 μm . Data are presented as means \pm SD, * P <0.05 and ** P <0.01; n.s. indicates no statistical significance.

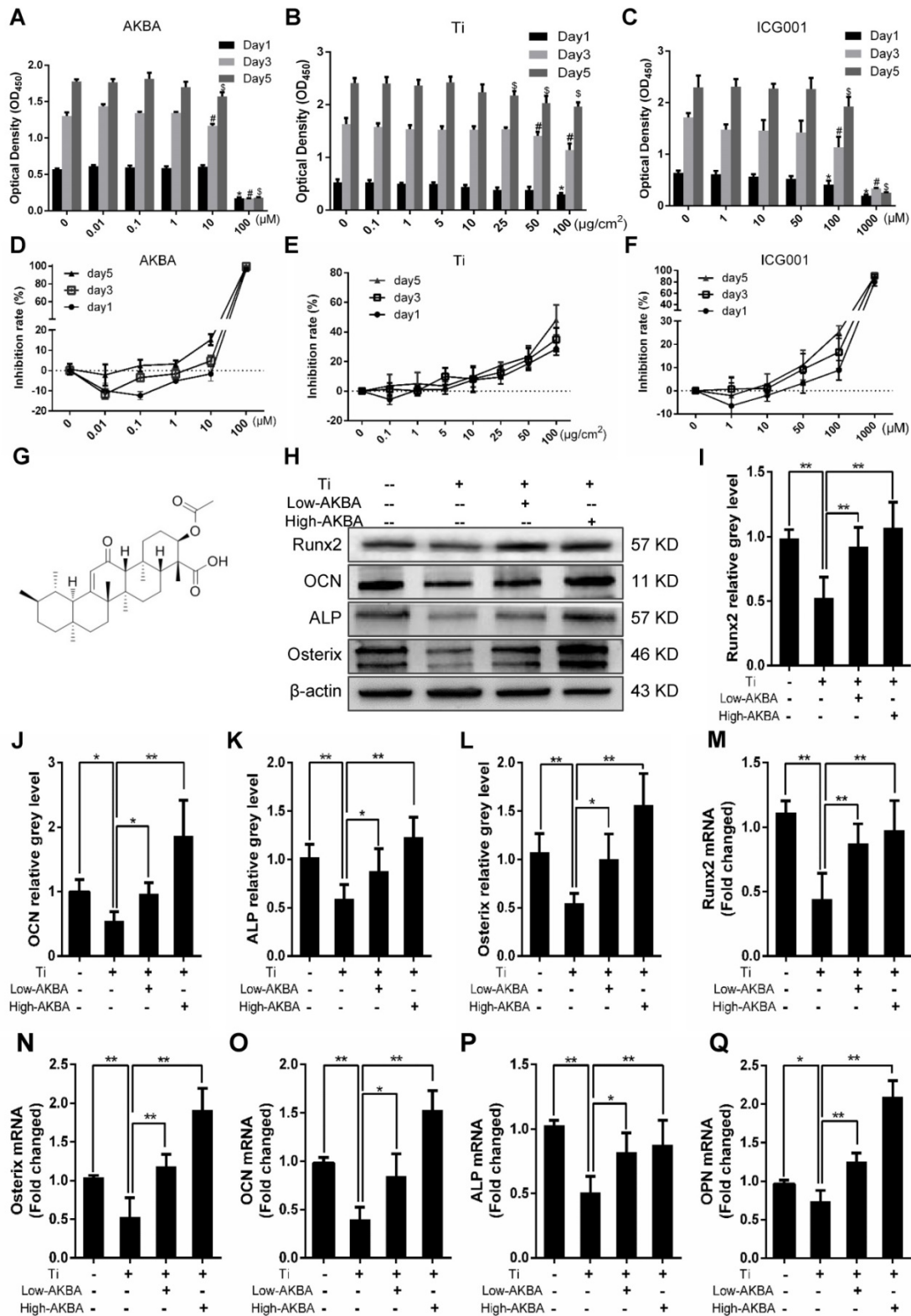


Figure 4. AKBA treatment attenuated titanium particle-induced inhibition of osteogenic differentiation in MC3T3-E1 cells. (A-C) Cell viability after 1, 3, or 5 days of treatment. Viability was determined using a CCK-8 assay. **P*<0.05, compared with 0 μM treatment (day 1), #*P*<0.05, compared with 0 μM treatment (day 3), and §*P*<0.05, compared with 0 μM treatment (day 5). (D-F) Inhibition rate of MC3T3-E1 cells. (G) Chemical structure of AKBA. (H-L) Runx2, OCN, Osterix, and ALP protein expression levels. (M-Q) Runx2, Osterix, OCN, ALP, and OPN mRNA expression levels. Cell differentiation was induced for 1 and 3 days in qRT-PCR and Western blotting, respectively. Relative grey levels were analyzed using Image J. Both low-AKBA (100 nM) group and high-AKBA (1000 nM) group contained 5 μg/cm² titanium particles. Data are presented as means ± SD. n=6: six samples were obtained from six wells in a single experiment for the CCK-8 assay. n=6: three samples were obtained from three independent experiments, and each sample was collected from three wells in a single experiment and analyzed in duplicates by Western blotting. n=9: three samples were obtained from three independent experiments, and each sample was collected from three wells in a single experiment and analyzed in triplicate by qRT-PCR. **P*<0.05 and ***P*<0.01, compared with the titanium particle group.

Differentiated MC3T3-E1 cells were stimulated by 5 $\mu\text{g}/\text{cm}^2$ titanium particles with or without low (100 nM) or high (1000 nM) concentrations of AKBA for 3 days. Western blot analysis showed that the expression of ALP, Osterix, OCN, and Runx2 was increased in AKBA-treated cells (Fig. 4H–L), indicating that treatment mitigated titanium-induced osteogenic reduction by enhancing the expression of osteogenic proteins. Also, the qRT-PCR analysis demonstrated that AKBA treatment resulted in a significant increase in the mRNA levels of runt-related transcription factor 2 (Runx2), Osterix, OCN, Osteopontin (OPN), and ALP (Fig. 4M–Q). ALP staining revealed that titanium particles inhibited the osteogenic differentiation of MC3T3-E1 cells which was alleviated by AKBA treatment in a dose-dependent manner (Fig. 5A and B). Consistent with this, Alizarin red S staining (ARS) demonstrated that 100 nM and 1000 nM AKBA treatment profoundly stimulated cell mineralization by approximately 224.3% and 324.3%, respectively, compared to cells treated with titanium particles only (Fig. 5C and D).

AKBA treatment alleviated titanium-induced osteogenic reduction in osteolysis by activating the GSK-3 β / β -catenin signaling pathway *in vitro* and *in vivo*

To investigate the potential molecular mechanisms underlying the osteogenic effects of AKBA treatment, we examined the expression of key markers involved in relevant signaling pathways and MC3T3-E1 differentiation. As expected, Western blot and qRT-PCR analyses showed that the expression of β -catenin and Axin-2 was inhibited by the titanium particles. However, β -catenin and Axin-2 levels were markedly increased in cells treated with AKBA compared to cells treated with titanium particles only. Western blot analysis of pSer9-GSK-3 β and GSK-3 β showed that AKBA treatment decreased the ratio of pSer9-GSK-3 β to GSK-3 β induced by titanium particles. These results indicated that the GSK-3 β / β -catenin signaling pathway may have mediated the protective effects of AKBA treatment (Fig. 6).

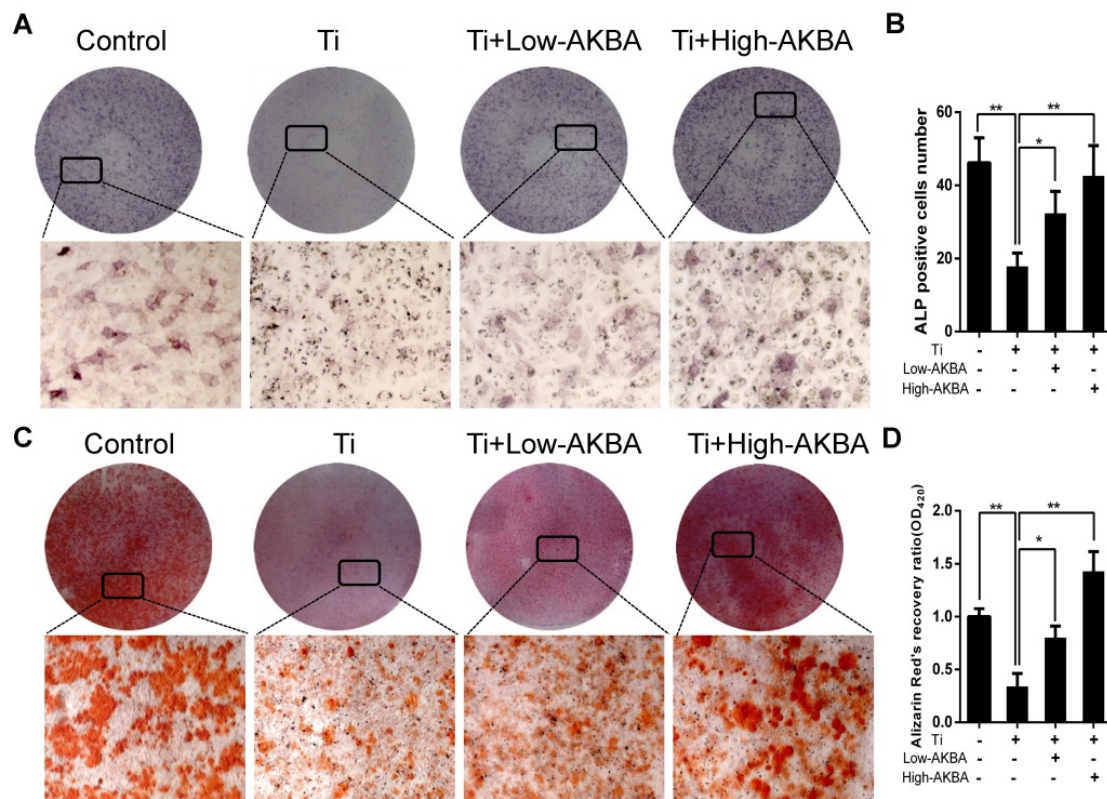


Figure 5. AKBA treatment alleviated titanium particle-induced inhibition of osteogenic differentiation and mineralization in MC3T3-E1 cells. (A) ALP staining at day 7 after osteogenic differentiation. (B) The number of ALP-positive cells in MC3T3-E1 cells. (C) Alizarin Red S (ARS) staining of MC3T3-E1 cells at day 14 after osteogenic differentiation. (D) Semi-quantitative analysis of ARS staining. Both low-AKBA (100 nM) group and high-AKBA (1000 nM) group contained 5 $\mu\text{g}/\text{cm}^2$ titanium particles. Data are presented as means \pm SD. $n = 9$: nine samples were obtained from three independent experiments, and each sample was collected from one well in a single experiment for the ALP staining and ARS staining. $n = 9$: three samples were obtained from three independent experiments, and each sample was collected from three wells in a single experiment and analyzed in triplicate for semi-quantitative analysis of ARS. * $P < 0.05$ and ** $P < 0.01$, compared with the titanium particle-treated group.

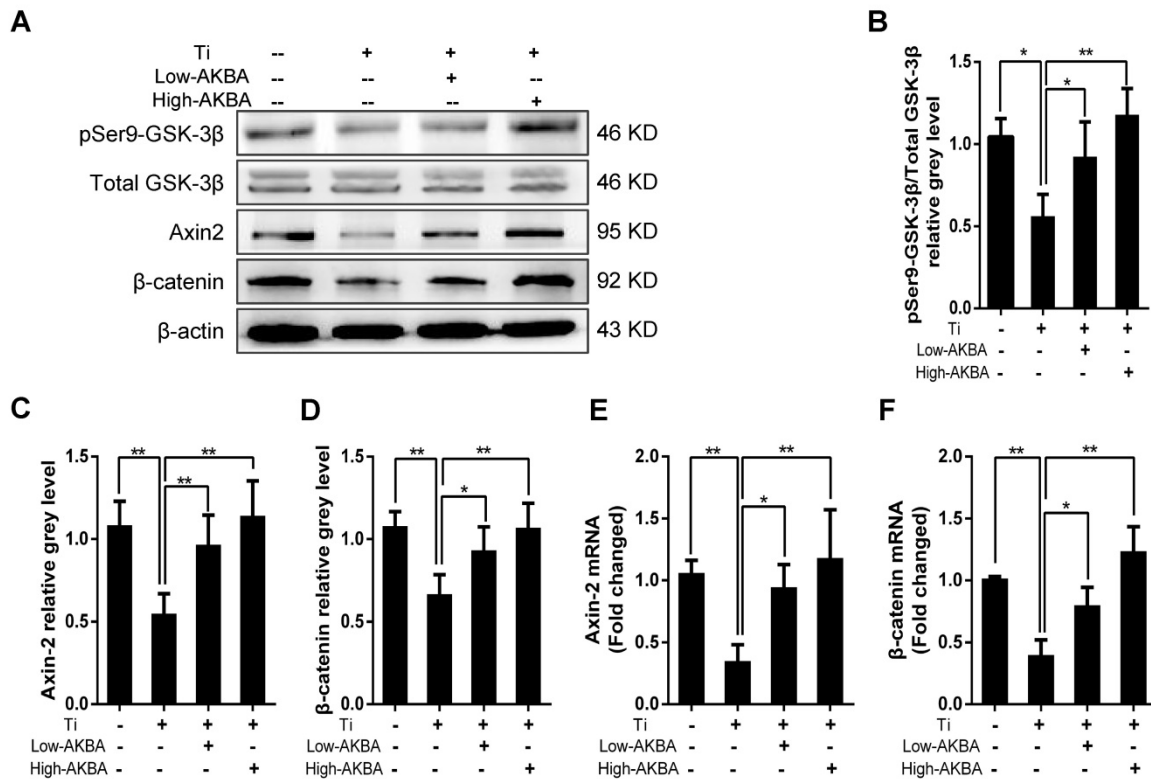


Figure 6. AKBA treatment rescued the titanium particle-induced inhibition of β -catenin in MC3T3-E1 cells. (A) Western blot analysis of expression levels of pSer9-GSK-3 β , β -catenin, and Axin-2. (B-D) The relative grey levels of pSer9-GSK-3 β /total-GSK-3 β , β -catenin, and Axin-2. (E, F) qRT-PCR analysis of the mRNA expression levels of pSer9-GSK-3 β , β -catenin, and Axin-2. Both low-AKBA (100 nM) group and high-AKBA (1000 nM) group contained 5 μ g/cm² titanium particles. Data are presented as means \pm SD. n=6 or 9 for Western blotting and qRT-PCR, respectively. * P <0.05 and ** P <0.01, compared with the titanium particle-treated group.

Indocyanine green-001 (ICG-001, Selleck), a specific inhibitor of the Wnt/ β -catenin signaling pathway, was used to verify the role of the GSK-3 β / β -catenin pathway. We first confirmed that ICG-001 could inhibit osteoblastic differentiation and mineralization via inhibiting Wnt/ β -catenin signaling pathway as shown in Fig. S1 and Fig. S2. Strikingly, treatment with 20 μ M ICG-001 (contained 5 μ g/cm² titanium particles and 1000 nM AKBA) abolished the AKBA-mediated rescue of the titanium particle-induced inhibition of the Wnt/ β -catenin signaling pathway. Western blot (Fig. 7A–C) and qRT-PCR (Fig. 7D and E) analyses indicated that ICG-001 inhibited the expression of β -catenin and Axin-2. Cellular immunofluorescence assays also indicated that AKBA treatment promoted the activation of β -catenin and increased its nuclear translocation. However, these effects were suppressed in the presence of ICG-001 (Fig. 7F).

Western blotting (Fig. 8A–E) and qRT-PCR (Fig. 8F–I) showed drastic decrease in the expression of osteogenic markers by ICG-001 treatment. As expected, ALP staining and the number of ALP-positive cells (Fig. 9A and B) were consistent with the number of calcium nodules detected by ARS staining, which were markedly reduced in cells

treated with ICG-001 compared to cells treated with AKBA alone (Fig. 9C and D). Overall, ICG-001 severely inhibited the protective effect of AKBA on β -catenin activity. These findings indicated that AKBA treatment alleviated the inhibition of the GSK-3 β / β -catenin signaling pathway caused by titanium particles, while ICG-001 treatment inhibited the protective effect of AKBA in titanium-induced osteogenic inhibition.

To further confirm that AKBA treatment improved titanium particle-induced osteogenic reduction via the GSK-3 β / β -catenin signaling pathway in murine calvaria, IHC staining of pSer9-GSK-3 β and β -catenin was performed. Intense pSer9-GSK-3 β and β -catenin staining was observed in AKBA-treated mice, compared with the low expression observed in the model mice (Fig. 10A and B). The semi-quantitative analysis showed that titanium particle-stimulation reduced the expression of β -catenin and pSer9-GSK-3 β compared with that in the control group. Treatment with AKBA reversed the effects of titanium particle stimulation (Fig. 10C and D). These data indicated that AKBA mitigated titanium-induced osteogenic reduction in osteolysis via activation of the GSK-3 β / β -catenin signaling pathway *in vivo*.

Discussion

Wear particles play an important biological role in the occurrence of PPO, an unavoidable problem that results in implant failure and revision surgery [33-35]. Proinflammatory and osteoclastogenic cytokines secreted by macrophages, fibroblasts, lymphocytes, and osteoclasts may break the balance between bone formation and bone resorption, resulting in PPO [36]. Previous studies have focused on anti-inflammatory, osteoclastogenesis, and biomaterial improvement [37-39]. However, inhibiting inflammation caused by wear particles

around the prosthesis has proven to be insufficient for the treatment of osteolysis [40]. Moreover, the direct exposure of osteoblasts to wear particles is another significant cause of PPO [16, 17, 41, 42]. Some studies have found that the expression levels of inflammatory and bone resorption factors were up-regulated and of bone formation-related factors down-regulated in osteoblasts exposed to wear particles, resulting in a decrease in osteogenesis [13, 14, 43]. Alleviating the wear particle-induced reduction of periprosthetic osteogenesis is a key factor in the prevention and treatment of PPO.

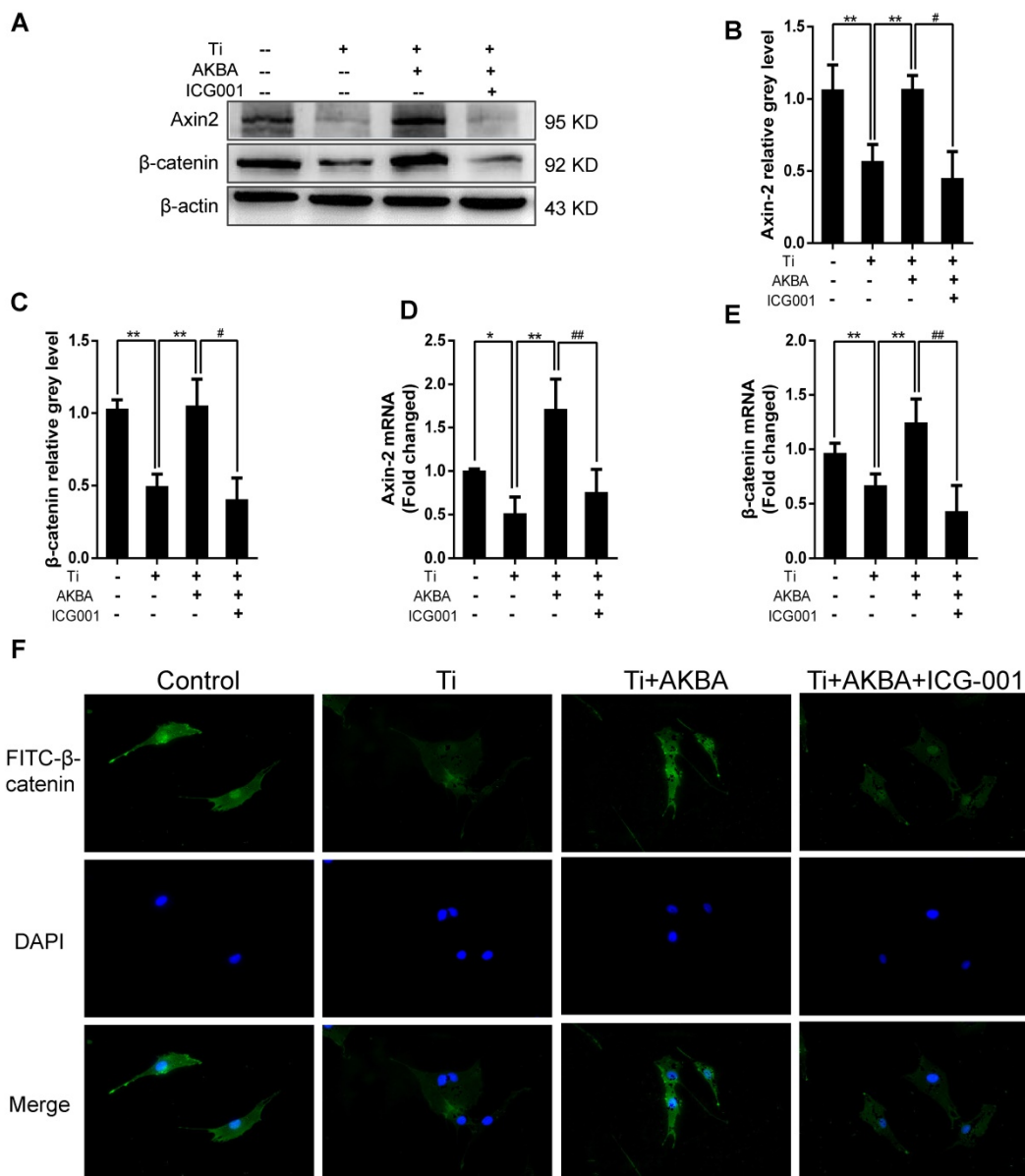


Figure 7. ICG-001 treatment reversed the effects of AKBA on the activity of β-catenin in MC3T3-E1 cells. (A-C) Western blot and (D, E) qRT-PCR analysis of the protein and mRNA levels of β-catenin and Axin-2. (F) Cellular immunofluorescence of β-catenin in MC3T3-E1 cells. Cell differentiation was induced for 24 h. AKBA group contained 5 μg/cm² titanium particles and 1000 nM AKBA, and ICG-001 group contained 5 μg/cm² titanium particles, 1000 nM AKBA and 20 μM ICG-001. Data are presented as means ± SD. n=6 or 9 for western blotting and qRT-PCR, respectively. n=9; nine samples were obtained from three independent experiments, and each sample was collected from one well in a single experiment for immunofluorescence assay. *P<0.05 and **P<0.01, compared with the model group. #P<0.05, ###P<0.01, compared with the AKBA treatment group.

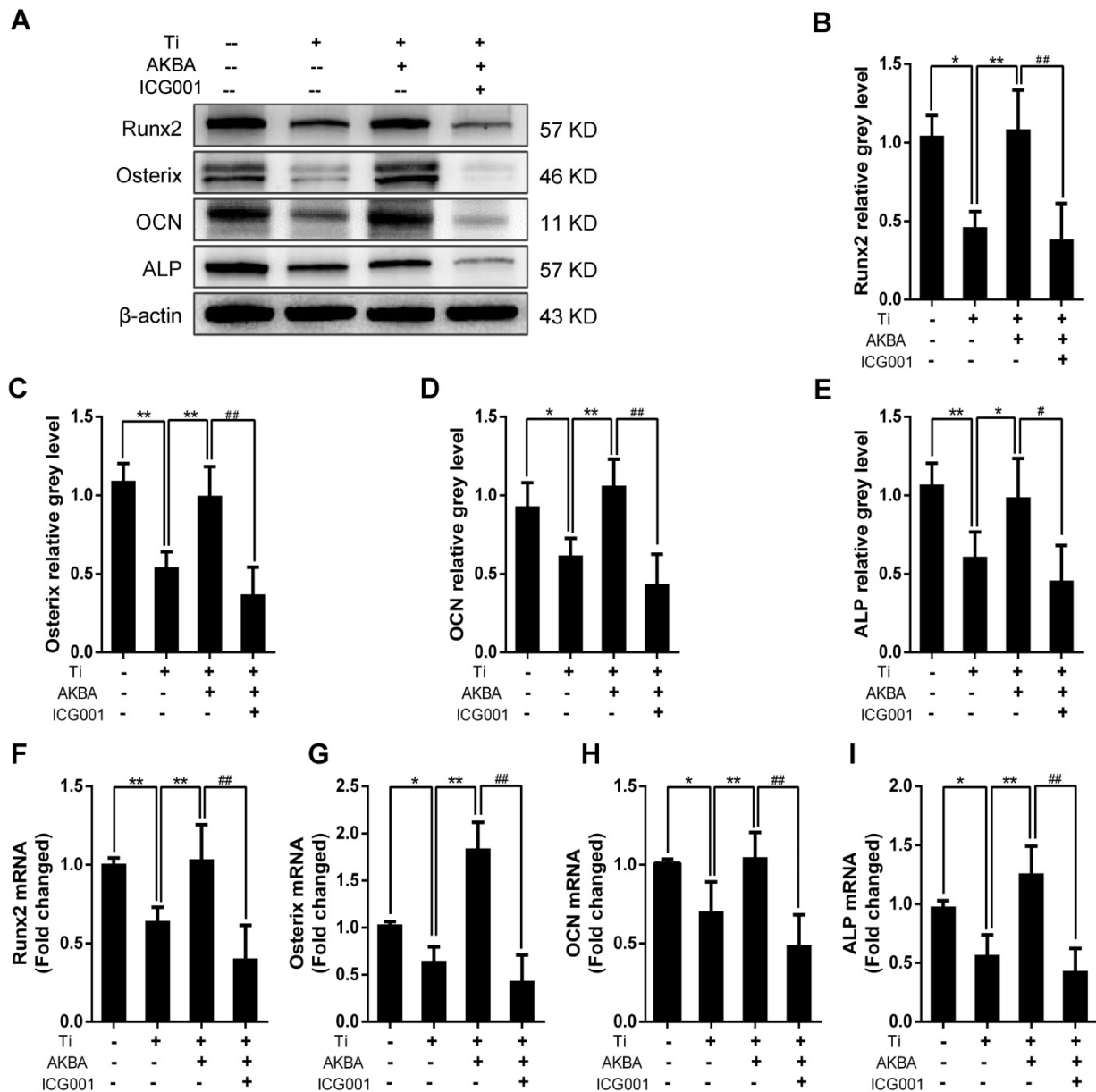


Figure 8. ICG-001 treatment reversed the effects of AKBA on osteogenic differentiation in MC3T3-E1. (A–E) Western blot analysis of expression levels of Runx2, Osterix, OCN, and ALP. (F–I) qRT-PCR analysis of the mRNA expression levels of Runx2, Osterix, OCN, and ALP. AKBA group contained 5 µg/cm² titanium particles and 1000 nM AKBA, and ICG-001 group contained 5 µg/cm² titanium particles, 1000 nM AKBA and 20 µM ICG-001. Data are presented as means ± SD. n=6 or 9 for western blot and qRT-PCR, respectively. *P<0.05 and **P<0.01, compared with the model group. #P<0.05 and ##P<0.01, compared with the AKBA treatment group.

BAs are pharmacologically active compounds of the pentacyclic triterpenes of different boswellia species. Thus far, over 12 kinds of BAs have been identified, though only KBA and AKBA have significant pharmacological activity [21]. AKBA, which is more active than KBA, has been found to inhibit host inflammatory response, mitigating inflammation-induced damage to cartilage, bronchial, and intestinal tissues. Furthermore, AKBA has known anti-tumor, anti-ulcer, anti-asthma, anti-oxidation, immunomodulatory, and lipid regulatory effects [18, 25]. AKBA treatment abolished osteoclastogenesis and promoted osteoblastic differentiation through the

regulation of NF-κB activity [27, 28]. In the current study, we observed that AKBA reversed titanium particle-induced inhibition of osteoblast formation. Also, we showed, for the first time, that AKBA mitigated titanium particle-induced osteolysis and stimulated osteogenesis.

Previous studies have reported that the Wnt/β-catenin signaling pathway plays a vital role in bone formation, and the activation of β-catenin has been shown to promote osteoblast proliferation, differentiation, and maturation [44-46]. The Wnt/β-catenin signaling pathway has been shown to be key to the homeostatic maintenance of bone tissue

and, as such, has become a promising target of osteoporosis and rheumatoid arthritis therapies [47, 48]. GSK-3 β , a serine/threonine protein kinase, plays a significant part in cell growth, differentiation, apoptosis, stem cell maintenance, and tumor formation [16, 49]. Also, GSK-3 β can phosphorylate β -catenin, causing its inactivation and degradation in the cytoplasm. Inhibition of GSK-3 β by phosphorylation of Ser9 can activate the classical Wnt/ β -catenin signaling pathway, further improving osteogenesis [16, 50, 51]. Our study showed that AKBA treatment resulted in marked activation of the GSK-3 β / β -catenin signaling pathway and mitigated titanium particle-induced osteogenic inhibition. Western blot, qRT-PCR, and IHC analyses further demonstrated that AKBA treatment significantly up-regulated the expression of β -catenin, Axin-2, and inactivated GSK-3 β through phosphorylation at Ser 9.

ICG-001, which specifically binds the cAMP-response element binding protein (CREB)-binding protein (CBP) to disrupt its interaction with β -catenin and inhibit CBP function as a coactivator of Wnt/ β -catenin-mediated transcription [52, 53], impaired the osteogenic function of MC3T3-E1 cells. Immunofluorescence analysis indicated that AKBA treatment promoted nuclear translocation of β -catenin following titanium particle-induced cytoplasmic localization. However, ICG-001 treatment reversed the effects of AKBA on the activity of β -catenin in MC3T3-E1 cells.

Collectively, these results demonstrated that AKBA treatment alleviated the titanium-induced inhibition of bone regeneration via activation of the GSK-3 β / β -catenin signaling pathway.

In our previous study, we reported that titanium particles inhibited osteoblastic function and induced bone destruction by regulating GSK-3 β that could be alleviated by lithium chloride, a selective inhibitor of GSK-3 β . However, GSK-3 β , a serine/threonine protein kinase, plays a significant role in numerous vital biological processes, and deletion of GSK-3 β gene impaired synaptic plasticity and memory, leading to hypertrophic cardiomyopathy and even death during embryonic development [54-56]. Besides, the long-term clinical application of lithium chloride as an inhibitor of GSK-3 β is accompanied by acute toxic effects [57, 58]. In our current study, we observed that AKBA eased osteolysis by enhancing bone formation, which may be associated with the regulation of GSK-3 β . However, the involvement of other osteogenic signaling pathways cannot be ruled out and should be investigated in the future. Additionally, inflammation and osteoclastic resorption are two key factors involved in PPO. Some studies have shown that AKBA has anti-inflammatory effect and regulation of osteogenic and osteoclastogenic functions [27, 28, 59]. Thus, AKBA may be a promising drug to prevent and treat PPO by enhancing osteogenesis and anti-inflammatory impact as well as inhibiting osteoclastogenesis.

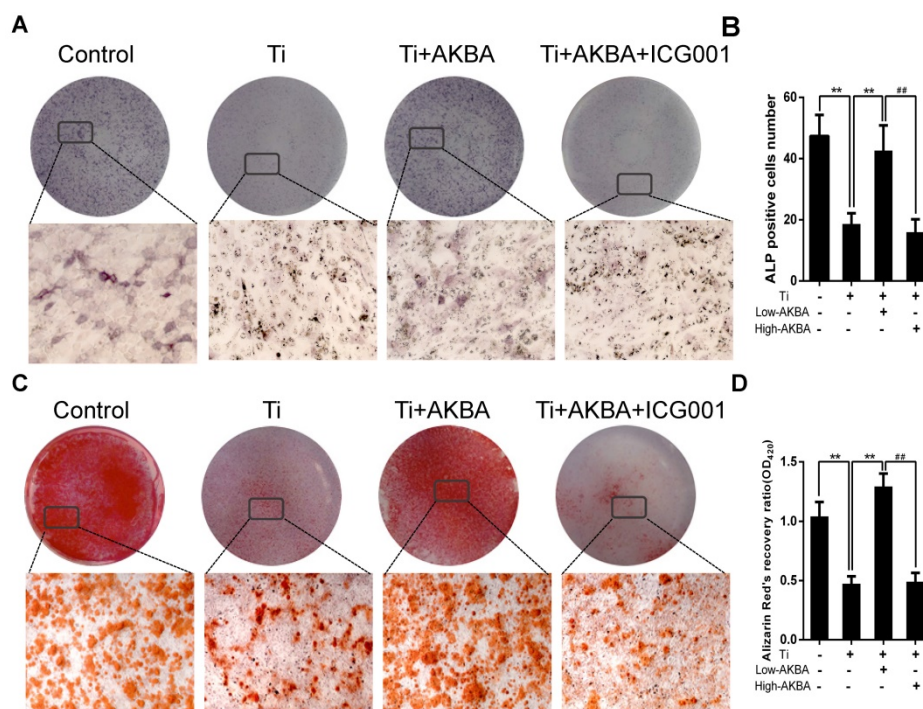


Figure 9. ICG-001 treatment reversed the effects of AKBA on osteogenic differentiation and mineralization in MC3T3-E1. (A) ALP staining in MC3T3-E1 cells. (B) The number of ALP-positive cells. (C) ARS staining in MC3T3-E1 cells. (D) Semi-quantitative analysis of ARS staining. AKBA group contained 5 $\mu\text{g}/\text{cm}^2$ titanium particles, 1000 nM AKBA, and ICG-001 group contained 5 $\mu\text{g}/\text{cm}^2$ titanium particles, 1000 nM AKBA and 20 μM ICG-001. Data are presented as means \pm SD, $n = 9$ for ALP staining, ARS staining and semi-quantitative analysis of ARS. * $P < 0.05$ and ** $P < 0.01$, compared with the model group. # $P < 0.05$ and ## $P < 0.01$, compared with the AKBA treatment group.

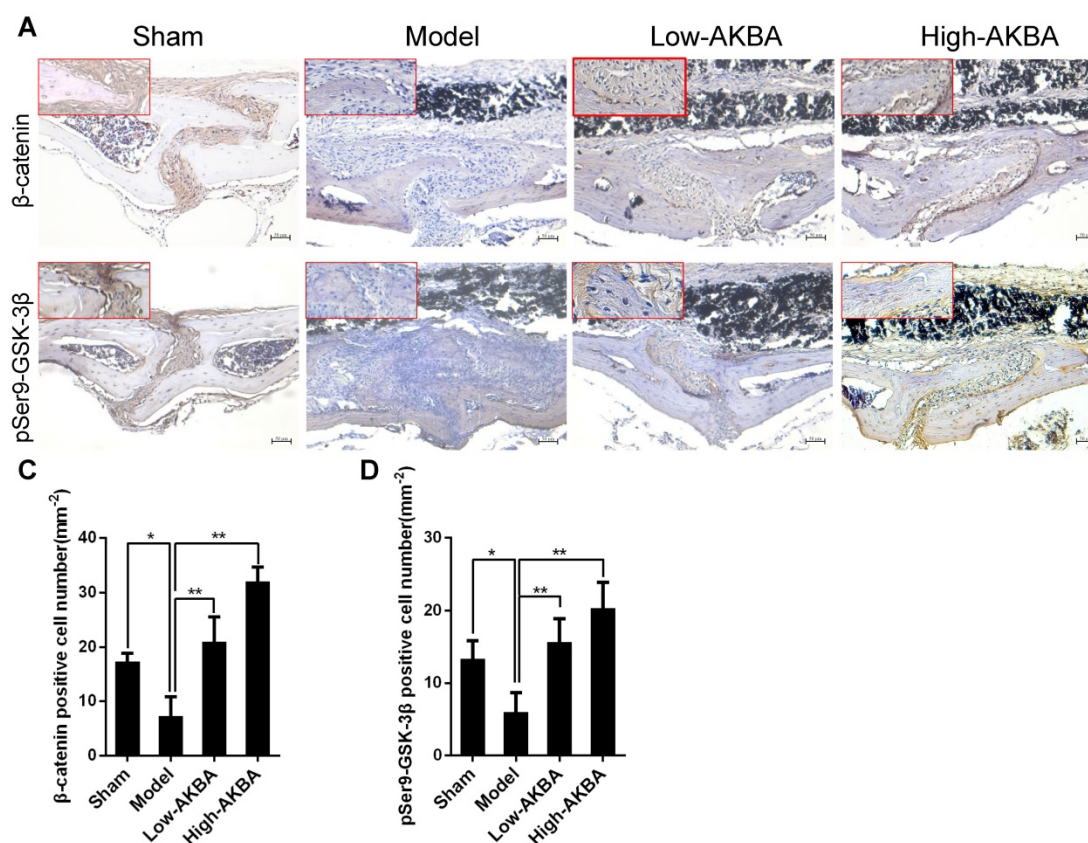


Figure 10. AKBA treatment activated the GSK-3β/β-catenin signaling pathway *in vivo*. (A, B) IHC analysis of the expression of pSer9-GSK-3β and β-catenin. (C, D) Quantification of the number of positive cells. Both low-AKBA (5 mg/kg per day) group and high-AKBA (5 mg/kg per day) group contained 20 mg titanium particles titanium particles. n=5 per group. Scale bar=50 μm. Data are presented as means ± SD. *P<0.05 and **P<0.01.

In the future, we plan to further explore various molecular aspects of AKBA's positive impact on osteogenesis. For example, TRAP staining showed that AKBA treatment could reduce the number of osteoclasts surrounding osteolytic areas. Besides, osteoblasts could enhance the expression and secretion of OPG via Wnt/β-catenin signaling pathway, and subsequently suppress osteoclastogenesis via OPG/RANKL/RANK pathway [60]. It would, therefore, be essential to get a better understanding of the direct and/or indirect regulation of osteoclasts by AKBA to attenuate titanium particle-induced osteolysis. Also, inflammation plays a key role in titanium-induced osteolysis, and inflammatory cytokines could not only enhance osteolysis directly, but could inhibit osteogenesis by suppressing the expression of collagen I and osteocalcin [13, 61, 62]. AKBA has been shown to exert anti-inflammatory effects on other tissues including bone and cartilage tissues [23, 63]. Thus, it is important to clarify the potential anti-inflammatory role of AKBA in mitigating titanium-induced osteolysis. Finally, in our current study, we observed that AKBA eased osteolysis by enhancing bone formation, which may be associated with the regulation of GSK-3β/β-catenin signaling

pathway. However, the involvement of other osteogenic signaling pathways cannot be ruled out and should be investigated in the future.

Conclusion

Our study explored the effect of AKBA treatment on osteogenic reduction in titanium-induced osteolysis. AKBA treatment was found to attenuate titanium-induced osteogenic inhibition which was regulated through the activation of the GSK-3β/β-catenin signaling pathway (Graphical Abstract). These results provide a deeper insight into whether and how AKBA regulates bone metabolism and demonstrate that AKBA is a potential new target for the treatment of wear particle-induced PPO.

Supplementary Material

Supplementary figures and tables.

<http://www.thno.org/v09p7140s1.pdf>

Abbreviations

ABA: β-BA-derivative acetyl-boswellic acid; AKBA: acetyl-11-keto-β-boswellic acid; ALP: alkaline phosphatase; α-BA: Alpha-boswellic acid; α-MEM:

Alpha-Minimum Essential Medium; BA: boswellic acid; BCIP/NBT: 5-bromo-4-chloro-3-indolyl-phosphate/nitro blue tetrazolium; BES: bone eroded surface; BMD: bone mineral density; BT: bone thickness; BV: bone volume; BV/TV: bone volume/tissue volume; β -BA: beta-boswellic acid; CREB: cAMP-response element binding protein; DMEM: Dulbecco's Modified Eagle Medium; DMSO: dimethyl sulfoxide; ECL: enhanced chemiluminescence; EDTA: ethylene diamine tetraacetic acid; GADPH: glyceraldehyde-3-phosphate dehydrogenase; GSK-3 β : glycogen synthase kinase-3 β ; H&E: hematoxylin and eosin; ICG-001: indocyanine green-001; IHC: immunohistochemistry; IL-1 β : interleukin 1 β ; KBA: 11-keto- β -boswellic acid; MAR: mineral apposition rate; NF- κ B: nuclear factor- κ B; N.Oc/BS: the average number of osteoclasts to bone surface; OCN: osteocalcin; Oc.S/OB: the ratio of osteoclast surface-to-bone surface; OPN: osteopontin; PBS: phosphate buffered saline; PPO: peri-prosthetic osteolysis; qRT-PCR: quantitative real-time polymerase chain reaction; RANKL/RANK/OPG: receptor activator for nuclear factor- κ B ligand/receptor activator for nuclear factor- κ B/osteoprotegerin; RIPA: radio immunoprecipitation assay; Runx2: runt-related transcription factor 2; TJA: total joint arthroplasty; TNF- α : tumor necrosis factor- α ; TRAP: tartrate-resistant acid phosphatase.

Acknowledgements

This research was supported by the National Nature Science Foundation of China (81873990, 81873991, 81672238, 81472077, 81472105 and 81372018), the Jiangsu Provincial Medical Youth Talent (QNRC2016751), the Natural Science Foundation of Jiangsu province (BK20180001), Changshu Science and Technology Development Plan Project 2018 (CS201819) and Special Project of Diagnosis and Treatment Technology for Key Clinical Diseases in Suzhou in 2018 (LCZX201824), the Priority Academic Program Development of Jiangsu Higher Education Institutions (PAPD).

Contributions

Dechun Geng, Jun Zhou and Yaozeng Xu contributed to experimental conception and design, supervising the research group and revising manuscript as corresponding author; Longbin Xiong, Yu Liu, Feng Zhu, Jiayi Lin, Dongxiang Wen and Zhen Wang made substantial contributions to designing experimental plans, and did most of experiments in vivo and vitro, data acquiring and analyzing, in addition, manuscript writing and revising; Jiaxiang Bai, Gaoran Ge, Congxin Xu and Ye Gu were contributed to performing micro-CT, TRAP

staining and relative data analysis and involved in guidance of experimental method and figures adjustment.

Competing Interests

The authors have declared that no competing interest exists.

References

- Della Valle CJ, Mesko NW, Quigley L, Rosenberg AG, Jacobs JJ, Galante JO. Primary total hip arthroplasty with a porous-coated acetabular component. A concise follow-up, at a minimum of twenty years, of previous reports. *J Bone Joint Surg Am.* 2009; 91: 1130-5.
- Holt G, Murnaghan C, Reilly J, Meek RM. The biology of aseptic osteolysis. *Clin Orthop Relat Res.* 2007; 460: 240-52.
- Stea S, Visentin M, Granchi D, Ciapetti G, Donati ME, Sudanese A, et al. Cytokines and osteolysis around total hip prostheses. *Cytokine.* 2000; 12: 1575-9.
- Holding CA, Findlay DM, Stamenkov R, Neale SD, Lucas H, Dharmapatri AS, et al. The correlation of RANK, RANKL and TNF α expression with bone loss volume and polyethylene wear debris around hip implants. *Biomaterials.* 2006; 27: 5212-9.
- Chen M, Chen PM, Dong QR, Huang Q, She C, Xu W. p38 Signaling in titanium particle-induced MMP-2 secretion and activation in differentiating MC3T3-E1 cells. *J Biomed Mater Res A.* 2014; 102: 2824-32.
- Wang Z, Liu N, Liu K, Zhou G, Gan J, Wang Z, et al. Autophagy mediated CoCrMo particle-induced peri-implant osteolysis by promoting osteoblast apoptosis. *Autophagy.* 2015; 11: 2358-69.
- Klinder A, Seyfarth A, Hansmann D, Bader R, Jonitz-Heincke A. Inflammatory Response of Human Peripheral Blood Mononuclear Cells and Osteoblasts Incubated With Metallic and Ceramic Submicron Particles. *Front Immunol.* 2018; 9: 831.
- Drynda A, Drynda S, Kekow J, Lohmann CH, Bertrand J. Differential Effect of Cobalt and Chromium Ions as Well as CoCr Particles on the Expression of Osteogenic Markers and Osteoblast Function. *Int J Mol Sci.* 2018; 19 (10): 3034.
- Gong ZM, Tang ZY, Sun XL. LncRNA PRNCR1 regulates CXCR4 expression to affect osteogenic differentiation and contribute to osteolysis after hip replacement. *Gene.* 2018; 673: 251-61.
- O'Neill SC, Queally JM, Devitt BM, Doran PP, O'Byrne JM. The role of osteoblasts in peri-prosthetic osteolysis. *Bone Joint J.* 2013; 95-b: 1022-6.
- Markhoff J, Weinmann M, Schulze C, Bader R. Influence of different grained powders and pellets made of Niobium and Ti-42Nb on human cell viability. *Mater Sci Eng C Mater Biol Appl.* 2017; 73: 756-66.
- Atkins GJ, Wellton KJ, Holding CA, Haynes DR, Howie DW, Findlay DM. The induction of a catabolic phenotype in human primary osteoblasts and osteocytes by polyethylene particles. *Biomaterials.* 2009; 30: 3672-81.
- Jonitz-Heincke A, Lochner K, Schulze C, Pohle D, Pustlank W, Hansmann D, et al. Contribution of human osteoblasts and macrophages to bone matrix degradation and proinflammatory cytokine release after exposure to abrasive endoprosthetic wear particles. *Mol Med Rep.* 2016; 14: 1491-500.
- Lee SS, Sharma AR, Choi BS, Jung JS, Chang JD, Park S, et al. The effect of TNF α secreted from macrophages activated by titanium particles on osteogenic activity regulated by WNT/BMP signaling in osteoprogenitor cells. *Biomaterials.* 2012; 33: 4251-63.
- Gallo J, Goodman SB, Kontinen YT, Raska M. Particle disease: biologic mechanisms of periprosthetic osteolysis in total hip arthroplasty. *Innate Immun.* 2013; 19: 213-24.
- Gu Y, Wang Z, Shi J, Wang L, Hou Z, Guo X, et al. Titanium particle-induced osteogenic inhibition and bone destruction are mediated by the GSK-3 β /beta-catenin signal pathway. *Cell Death Dis.* 2017; 8: e2878.
- Nam JS, Sharma A, Jagga S, Lee DH, Sharma G, Nguyen LT, et al. Suppression of osteogenic activity by regulation of WNT and BMP signaling during titanium particle induced osteolysis. *J Biomed Mater Res A.* 2017; 105: 912-26.
- Ammon HP. Boswellic Acids and Their Role in Chronic Inflammatory Diseases. *Adv Exp Med Biol.* 2016; 928: 291-327.
- Beghelli D, Isani G, Roncada P, Andreani G, Bistoni O, Bertocchi M, et al. Antioxidant and Ex Vivo Immune System Regulatory Properties of Boswellia serrata Extracts. *Oxid Med Cell Longev.* 2017; 2017: 7468064.
- Rehman NU, Ali L, Al-Harrasi A, Mabood F, Al-Broumi M, Khan AL, et al. Quantification of AKBA in Boswellia sacra Using NIRS Coupled with PLSR as an Alternative Method and Cross-Validation by HPLC. *Phytochem Anal.* 2018; 29: 137-43.
- Anthoni C, Laukoetter MG, Rijcken E, Vowinkel T, Mennigen R, Muller S, et al. Mechanisms underlying the anti-inflammatory actions of boswellic acid derivatives in experimental colitis. *Am J Physiol Gastrointest Liver Physiol.* 2006; 290: G1131-7.
- Taylor KM, Irving PM. Optimization of conventional therapy in patients with IBD. *Nat Rev Gastroenterol Hepatol.* 2011; 8: 646-56.

23. Catanzaro D, Rancan S, Orso G, Dall'Acqua S, Brun P, Giron MC, et al. *Boswellia serrata* Preserves Intestinal Epithelial Barrier from Oxidative and Inflammatory Damage. *PLoS one*. 2015; 10: e0125375.
24. Pang X, Yi Z, Zhang X, Sung B, Qu W, Lian X, et al. Acetyl-11-keto-beta-boswellic acid inhibits prostate tumor growth by suppressing vascular endothelial growth factor receptor 2-mediated angiogenesis. *Cancer Res*. 2009; 69: 5893-900.
25. Liu JJ, Toy WC, Liu S, Cheng A, Lim BK, Subramaniam T, et al. Acetyl-keto-beta-boswellic acid induces lipolysis in mature adipocytes. *Biochem Biophys Res Commun*. 2013; 431: 192-6.
26. Karima O, Riaz G, Yousefi R, Movahedi AA. The enhancement effect of beta-boswellic acid on hippocampal neurites outgrowth and branching (an in vitro study). *Neuro Sci*. 2010; 31: 315-20.
27. Takada Y, Ichikawa H, Badmaev V, Aggarwal BB. Acetyl-11-keto-beta-boswellic acid potentiates apoptosis, inhibits invasion, and abolishes osteoclastogenesis by suppressing NF-kappa B and NF-kappa B-regulated gene expression. *J Immunol*. 2006; 176: 3127-40.
28. Bai F, Chen X, Yang H, Xu HG. Acetyl-11-Keto-beta-Boswellic Acid Promotes Osteoblast Differentiation by Inhibiting Tumor Necrosis Factor-alpha and Nuclear Factor-kappaB Activity. *J Craniofac Surg*. 2018; 29: 1996-2002.
29. Ding H, Zhu Z, Tang T, Yu D, Yu B, Dai K. Comparison of the cytotoxic and inflammatory responses of titanium particles with different methods for endotoxin removal in RAW264.7 macrophages. *J Mater Sci Mater Med*. 2012; 23: 1055-62.
30. von Knoch M, Jewison DE, Sibonga JD, Sprecher C, Morrey BF, Loer F, et al. The effectiveness of polyethylene versus titanium particles in inducing osteolysis in vivo. *J Orthop Res*. 2004; 22: 237-43.
31. Geng D, Xu Y, Yang H, Wang J, Zhu X, Zhu G, et al. Protection against titanium particle induced osteolysis by cannabinoid receptor 2 selective antagonist. *Biomaterials*. 2010; 31: 1996-2000.
32. Bustin S. The continuing problem of poor transparency of reporting and use of inappropriate methods for RT-qPCR. *Biomol Detect Quantif*. 2017; 12: 7-9.
33. Wang L, Guo X, Zhou W, Ding Y, Shi J, Wu X, et al. Protein phosphatase 2A as a new target for downregulating osteoclastogenesis and alleviating titanium particle-induced bone resorption. *Acta Biomater*. 2018; 73: 488-99.
34. Boeckstyns ME, Toxvaerd A, Bansal M, Vadstrup LS. Wear particles and osteolysis in patients with total wrist arthroplasty. *J Hand Surg Am*. 2014; 39: 2396-404.
35. Sukur E, Akman YE, Ozturkmen Y, Kucukdurmaz F. Particle Disease: A Current Review of the Biological Mechanisms in Periprosthetic Osteolysis After Hip Arthroplasty. *Open J Orthop*. 2016; 10: 241-51.
36. Xu J, Nyga A, Li W, Zhang X, Gavara N, Knight MM, et al. Cobalt ions stimulate a fibrotic response through matrix remodelling, fibroblast contraction and release of pro-fibrotic signals from macrophages. *Eur Cell Mater*. 2018; 36: 142-55.
37. Zaveri TD, Dolgova NV, Lewis JS, Hamaker K, Clare-Salzler MJ, Keselowsky BG. Macrophage integrins modulate response to ultra-high molecular weight polyethylene particles and direct particle-induced osteolysis. *Biomaterials*. 2017; 115: 128-40.
38. Espirito Santo AI, Ersek A, Freidin A, Feldmann M, Stoop AA, Horwood NJ. Selective inhibition of TNFR1 reduces osteoclast numbers and is differentiated from anti-TNF in a LPS-driven model of inflammatory bone loss. *Biochem Biophys Res Commun*. 2015; 464: 1145-50.
39. Zheng ZW, Chen YH, Wu DY, Wang JB, Lv MM, Wang XS, et al. Development of an Accurate and Proactive Immunomodulatory Strategy to Improve Bone Substitute Material-Mediated Osteogenesis and Angiogenesis. *Theranostics*. 2018; 8: 5482-500.
40. Noordin S, Masri B. Periprosthetic osteolysis: genetics, mechanisms and potential therapeutic interventions. *Can J Surg*. 2012; 55: 408-17.
41. Yao J, Cs-Szabo G, Jacobs JJ, Kuettner KE, Glant TT. Suppression of osteoblast function by titanium particles. *J Bone Joint Surg Am*. 1997; 79: 107-12.
42. Goodman SB, Ma T, Chiu R, Ramachandran R, Smith RL. Effects of orthopaedic wear particles on osteoprogenitor cells. *Biomaterials*. 2006; 27: 6096-101.
43. Kalbacova M, Roessler S, Hempel U, Tsaryk R, Peters K, Scharnweber D, et al. The effect of electrochemically simulated titanium cathodic corrosion products on ROS production and metabolic activity of osteoblasts and monocytes/macrophages. *Biomaterials*. 2007; 28: 3263-72.
44. Duan P, Bonewald LF. The role of the wnt/beta-catenin signaling pathway in formation and maintenance of bone and teeth. *Int J Biochem Cell Biol*. 2016; 77: 23-9.
45. Yodthong T, Kedjarune-Leggat U, Smythe C, Wititsuwannakul R, Pitakpompreecha T. I-Quebrachitol Promotes the Proliferation, Differentiation, and Mineralization of MC3T3-E1 Cells: Involvement of the BMP-2/Runx2/MAPK/Wnt/beta-Catenin Signaling Pathway. *Molecules*. 2018; 23 (12): 3086.
46. Wang J, Tao Y, Ping Z, Zhang W, Hu X, Wang Y, et al. Icaritin attenuates titanium-particle inhibition of bone formation by activating the Wnt/beta-catenin signaling pathway in vivo and in vitro. *Sci Rep*. 2016; 6: 23827.
47. Krajewska-Wlodarczyk M, Stompor T. Osteoporosis and vascular calcification in rheumatoid arthritis - the role of osteoprotegerin and sclerostin. *Pol Merkuri Lekarski*. 2017; 43: 41-7.
48. Adami G, Orsolini G, Adami S, Viapiana O, Idolazzi L, Gatti D, et al. Effects of TNF Inhibitors on Parathyroid Hormone and Wnt Signaling Antagonists in Rheumatoid Arthritis. *Calcif Tissue Int*. 2016; 99: 360-4.
49. Antika LD, Lee EJ, Kim YH, Kang MK, Park SH, Kim DY, et al. Dietary phlorizin enhances osteoblastogenic bone formation through enhancing beta-catenin activity via GSK-3beta inhibition in a model of senile osteoporosis. *J Nutr Biochem*. 2017; 49: 42-52.
50. McCubrey JA, Rakus D, Gizak A, Steelman LS, Abrams SL, Lertpiriyapong K, et al. Effects of mutations in Wnt/beta-catenin, hedgehog, Notch and PI3K pathways on GSK-3 activity-Diverse effects on cell growth, metabolism and cancer. *Biochim Biophys Acta*. 2016; 1863: 2942-76.
51. Li VS, Ng SS, Boersema PJ, Low TY, Karthaus WR, Gerlach JP, et al. Wnt signaling through inhibition of beta-catenin degradation in an intact Axin1 complex. *Cell*. 2012; 149: 1245-56.
52. Emami KH, Nguyen C, Ma H, Kim DH, Jeong KW, Eguchi M, et al. A small molecule inhibitor of beta-catenin/CREB-binding protein transcription [corrected]. *Proc Natl Acad Sci U S A*. 2004; 101: 12682-7.
53. Arensman MD, Telesca D, Lay AR, Kershaw KM, Wu N, Donahue TR, et al. The CREB-binding protein inhibitor ICG-001 suppresses pancreatic cancer growth. *Mol Cancer Ther*. 2014; 13: 2303-14.
54. Wen J, Yan H, He M, Zhang T, Mu X, Wang H, et al. GSK-3beta protects fetal oocytes from premature death via modulating TAP63 expression in mice. *BMC Biol*. 2019; 17 (1): 23.
55. Liu E, Xie AJ, Zhou Q, Li M, Zhang S, Li S, et al. GSK-3beta deletion in dentate gyrus excitatory neuron impairs synaptic plasticity and memory. *Sci Rep*. 2017; 7: 5781.
56. Kerkela R, Kockeritz L, Macaulay K, Zhou J, Doble BW, Beahm C, et al. Deletion of GSK-3beta in mice leads to hypertrophic cardiomyopathy secondary to cardiomyoblast hyperproliferation. *J Clin Invest*. 2008; 118: 3609-18.
57. Patil V, Gupta R, Verma R, Balhara YP. Neuroleptic Malignant Syndrome Associated with Lithium Toxicity. *Oman Med J*. 2016; 31: 309-11.
58. Pardina-Vilella L, Garcia-Gorostiaga I, Azkune-Calle I, Vicente-Olabarria I, Martinez-Arroyo A, Bocos-Portillo J, et al. Reversible alterations in the dentate nuclei and rapid-onset cerebral atrophy due to neurotoxicity caused by lithium. *Rev Neurol*. 2017; 65: 223-5.
59. Sengupta K, Alluri KV, Satish AR, Mishra S, Golakoti T, Sarma KV, et al. A double blind, randomized, placebo controlled study of the efficacy and safety of 5-Loxin for treatment of osteoarthritis of the knee. *Arthritis Res Ther*. 2008; 10: R85.
60. Glass DA, Bialek P, Ahn JD, Starbuck M, Patel MS, Clevers H, et al. Canonical Wnt signaling in differentiated osteoblasts controls osteoclast differentiation. *Dev Cell*. 2005; 8: 751-64.
61. Jablonski H, Rekasi H, Jager M. The influence of calcitonin gene-related peptide on markers of bone metabolism in MG-63 osteoblast-like cells co-cultured with THP-1 macrophage-like cells under virtually osteolytic conditions. *BMC Musculoskelet Disord*. 2016; 17: 199.
62. Mediero A, Frenkel SR, Wilder T, He W, Mazumder A, Cronstein BN. Adenosine A2A receptor activation prevents wear particle-induced osteolysis. *Sci Transl Med*. 2012; 4: 135-65.
63. Mostafa DM, Ammar NM, Abd El-Alim SH, Kassem AA, Hussein RA, Awad G, et al. *Boswellia carterii* liquisolid systems with promoted anti-inflammatory activity. *Curr Drug Deliv*. 2015; 12: 454-63.